Effect of backwashing on activated carbon adsorption using plug flow pore surface diffusion model

Seongho Hong[†] and R. Scott Summers*

Department of Chemical & Environmental Engineering, Soongsil University, Seoul 156-743, Korea
*Dept. of Civil, Environmental and Architectural Engineering, University of Colorado, Boulder, CO 80309-0428, USA

Abstract–A fixed bed is gradually exhausted from top to bottom without backwashing; however, backwashing can rearrange the concentration gradient in the bed. After backwashing, saturated particles which are located at the top of the bed are homogeneously distributed in the bed. The used model to predict adsorption and backwashing effect of organic component is the plug flow pore surface diffusion model (PFPSDM). A sensitivity analysis was performed to determine which parameters have the greatest impact on the model results for components which can represent various organics. In addition, the effects of backwashing were examined by rearranging concentration gradient. For single component sensitivity analysis, the molecular weight was an important parameter. The breakthrough of the smaller molecular weight component was impacted more by backwashing. The SPDFR showed a significant impact on the breakthrough pattern. When surface diffusion was the dominant mechanism, high SPDFR, the breakthrough profile was sharper than when pore diffusion was dominant, low SPDFR. The adsorbability was an important parameter in determining the breakthrough pattern. As expected, the strongly adsorbable component showed the later breakthrough. Backwashing yielded earlier breakthrough for all single components and multi-components examined.

Key words: GAC, Adsorption, Backwashing, NOM, Freundlich Isotherm

INTRODUCTION

Adsorption of organic components on activated carbon is an interfacial phenomenon which is driven by concentration difference or gradient of solute at a phase boundary compared to a bulk solution. In the activated carbon adsorption, the interface is the pores or surfaces which exist outside or inside of the carbon particles. The pore consists of very complex channels of inside of the particles. Accordingly, an adsorbate should penetrate from bulk solution into the inner structure of activated carbon particles before it reaches an interfacial surface. Therefore, activated carbon adsorption is known as a mass transfer or transfer phenomenon.

Once an adsorbate has diffused from the bulk solution to the surface of the adsorbent, it can either adsorb or diffuse to the inside of the adsorbent. The high internal surface area of the adsorbent causes a concentration gradient for the adsorbate, which is the driving force for the flux. The internal mass transfer step can proceed within the fluid void space contained within the pores, which is referred to as pore diffusion, or along the surface walls of the pores as adsorbed molecules, which is referred to as surface diffusion [Sontheimer et al., 1988]. Thus, the overall mass transfer incorporates two intraparticle mechanisms and one external mechanism, which can be used to describe the adsorption kinetics in a fixed bed adsorber.

There are many models to predict adsorption behaviors on activated carbon. Homogeneous surface diffusion model (HSDM) is one of the well known models to predict adsorption of organic components onto activated carbon. However, the HSDM does not consider the pore diffusion.

The other model to predict adsorption of organic component is the plug flow pore surface diffusion model (PFPSDM). The model considers that the diffusion is divided into pore and surface diffusion. Therefore, the PFPSDM can predict adsorption behavior more precisely if the diffusion is incorporated with pore diffusion. Organic compounds in source water for drinking water treatment are very complex. It is necessary to understand the multicomponent adsorption to remove the organics in drinking water treatment. In addition, backwashing of the fixed bed is very common in drinking water treatment to reduce headloss caused by accumulation of particles or biomass in the bed. However, the effect of backwashing has not been investigated for single component and multi-component. On the other hand, activated carbon adsorption with attached biofilm is sometimes used in water and wastewater treatment [Shim et al., 2004; Kim et al., 2002].

In this study, a sensitivity analysis was investigated to determine which parameters have the greatest impact on the model results for components, which can represent various organics. In addition, the effect of backwashing was observed for single component and multi-components organics. The parameters used in this study include molecular weight, surface pore diffusion flux ratio (SPDFR), adsorbability and backwashing frequency for a single component. In addition, ratio of fictive component was used for multi-component.

MODEL DEVELOPMENT FOR THE PFPSDM

The equations describing the PFPSDM in a fixed bed adsorber are presented. In this study, the general equations are developed in dimensional form; the dimensionless forms are described by [Vaith, 1988; Vaith et al., 1988]. The assumptions incorporated into the PFPSDM are as follows: 1) the liquid phase flux is described by the linear

---

[†]To whom correspondence should be addressed.
E-mail: shong@ssu.ac.kr

driving force approximation, 2) the adsorption rate is very fast (local equilibrium), 3) the single component adsorption equilibrium is described by the single solute Freundlich isotherm equation, and the multi-component adsorption equilibrium is described by the single solute Freundlich isotherm equation with ideal adsorbed solution theory (IAST), 4) surface and pore diffusion describe the intraparticle mass flux and are independent of concentration, 5) there are no solute-solute interactions in the diffusion process, 6) the adsorbent particle is spherical, 7) solute transport in the axial direction occurs by advective flow, and 8) there is no radial dispersion or channeling.

To derive the overall mass balance for component in the fixed bed, a mass balance is written on a differential element in the bed. The adsorbate can be transferred into or out the differential element by advection and diffusion. The mass balance can be expressed in mathematical terms as follows:

$$\varepsilon v A [C_i(z,t) - C_i(z+\Delta z, t)] \Delta t - \varepsilon A D_{e,i} \left[\frac{\partial C_i(z,t)}{\partial z} - \frac{\partial C_i(z+\Delta z, t)}{\partial z} \right]$$
$$= \varepsilon A [C_i(z, t+\Delta t) - C_i(z,t)]$$
$$+ \rho_a (1-\varepsilon) A [q_{avg,i}(z, t+\Delta t) - q_{avg,i}(z,t)]$$
$$+ \left[\frac{\varepsilon_p}{\rho_a} C_{p,avg,i}(z, t+\Delta t) - \frac{\varepsilon_p}{\rho_a} C_{p,avg,i}(z,t) \right] \Delta z \quad (1)$$

in which, ε is the bed porosity; v is the interstitial velocity; ε_p is the void fraction of the pores within the adsorbent; A is the cross sectional area of the differential element; $C_i(z, t)$ is the liquid phase concentration of component i; $D_{e,i}$ is the axial eddy dispersivity based on the interstitial velocity of component i, ρ_a is the adsorbent density; $q_{avg}(z, t)$ is the average adsorbent phase concentration of the component; $C_{p,avg}$ is the average adsorbate concentration of the component in the adsorbent pores; z is the axial coordinate; and t is the elapsed time. The subscript, i, indicates each fictive component.

The average adsorbent phase concentration is given by;

$$q_{avg,i}(z,t) + \frac{\varepsilon_p}{\rho_a} C_{p,avg,i}(z,t) = \frac{3}{R^3} \int_0^R \left[q_i(r,z,t) - \frac{\varepsilon_p}{\rho_a} C_{p,i}(r,z,t) \right] r^2 dr \quad (2)$$

in which, R is the radius of the adsorbent; and r is the radial coordinate.

Dividing Eq. (1) by $A\Delta z \Delta t$ and taking the limits as Δz and Δt approach zero and substituting the Eq. (2) into Eq. (1) yields Eq. (3). Eq. (3) is the final form of the overall mass balance for component i in the fixed bed adsorber.

$$- v\varepsilon \frac{\partial C_i(z,t)}{\partial z} + \varepsilon D_{e,i} \frac{\partial^2 C_i(z,t)}{\partial z^2}$$
$$= \varepsilon \frac{\partial C_i(z,t)}{\partial t} + \frac{3\rho_a(1-\varepsilon)}{R^3} \frac{\partial}{\partial t} \int_0^R \left[q_i(z,r,t) + \frac{\varepsilon_p}{\rho_a} C_{p,i}(r,z,t) \right] r^2 dr \quad (3)$$

The dispersion term in Eq. (3) can be neglected based on initial model assumptions. Eq. (3) becomes a first order partial derivative with respect to z. In order to solve Eq. (3), one initial condition and one boundary condition are needed. The initial and boundary conditions are as follows:

$$C_i(0 \leq x \leq L, t=0)=0 \quad (4)$$

$$v[C_0 - C_i(z=L, t)] = \frac{\partial}{\partial t} \left[\int_0^t \left[C_i(z,t) \right. \right.$$
$$+ \left. \left. \frac{3\rho_a(1-\varepsilon)}{\varepsilon R^3} \int_0^R \left[q_i(r,z,t) + \frac{\varepsilon_p}{\rho_a} C_{p,i}(r,z,t) \right] r^2 dr \right] \right] dz \quad (5)$$

The liquid phase mass balance for the component is derived using the same differential element used in the previous development. The final form of the liquid phase mass balance for the component i in the fixed bed adsorber is:

$$- v \frac{\partial C_i(z,t)}{\partial z} = \frac{\partial C_i(z,t)}{\partial t} + \frac{3\beta_{L,i}(1-\varepsilon)}{R\varepsilon} [C_i(z,t) - C_{p,i}(r=R,z,t)] \quad (6)$$

in which, $C_{p,i}(r=R, z, t)$ is adsorbate concentration of component at the adsorbent surface and β_L is the external mass transfer coefficient. The final form of the intraparticle mass balance for the component i is given by Eq. (7).

$$\frac{1}{r^2} \frac{\partial}{\partial r} \left[r^2 D_{s,i} \frac{\partial q_i(r,z,t)}{\partial r} + r^2 \frac{D_{p,i}\varepsilon_p}{\rho_a} \frac{\partial C_{p,i}(r,z,t)}{\partial r} \right]$$
$$= \frac{\partial}{\partial t} \left[q_i(r,z,t) + \frac{\varepsilon_p}{\rho_a} C_{p,i}(r,z,t) \right] \quad (7)$$

in which, D_s is the surface diffusion coefficient and D_p is the pore diffusion coefficient of the component. The initial condition assumes that there is no adsorbate in the adsorbent initially. The initial condition for Eq. (7) is:

$$\left(q_i(r,z,t) + \frac{\varepsilon_p}{\rho_a} C_{p,i}(r,z,t) \right) \quad (0 \leq r \leq R, 0 \leq z \leq L, t=0)=0 \quad (8)$$

The following equations are the boundary conditions for Eq. (7).

$$\frac{\partial}{\partial r} \left[\left(q_i + \frac{\varepsilon_p}{\rho_a} C_{p,i} \right)(r=0, 0 \leq z \leq L, t=0) \right] = 0 \quad (9)$$

$$\frac{\partial}{\partial t} \int_0^R \left[q_i(r,z,t) + \frac{\varepsilon_p}{\rho_a} C_{p,i}(r,z,t) \right] r^2 dr$$
$$= \frac{\beta_{L,i}R^2}{\rho_a} [C_i(z,t) - C_{p,i}(r=R,z,t)] \quad (10)$$

$$D_{s,i}\rho_a \frac{\partial q_i(r=R,z,t)}{\partial r} + D_{p,i}\varepsilon_a \frac{\partial C_{p,i}(r=R,z,t)}{\partial r}$$
$$= \beta_{L,i} [C_i(z,t) - C_{p,i}(r=R,z,t)] \quad (11)$$

The nonlinear equation which couples the liquid and intraparticle mass balances is the Freundlich isotherm equation; $q=KC^{1/n}$. The final result including the axial coordinate for the concentration of a single component is given by Randtke and Prausnitz [1972] and Randtke and Snoeyink [1983]

$$C_p(r,z,t) = \left(\frac{q(r,z,t)}{K} \right)^{1/n} \quad (12)$$

Applying the IAST, the final result including the axial coordinate for the concentration of a multi-component is given by:

$$C_{p,i}(r,z,t) = \frac{q_i(r,z,t)}{\sum_{j=1}^N q_j(r,z,t)} \left(\frac{\sum_{k=1}^N n_k q_k(r,z,t)}{n_i K_i} \right)^{n_i} \quad (13)$$

The pore diffusion coefficient is defined by Eq. (13) where τ is the tortuosity.

$$D_p = \frac{D_L \varepsilon_p}{\tau} \quad (14)$$

in which D_L is the liquid diffusivity. The surface diffusion coefficient, D_S, is a function of the empirically determined SPDFR.

$$D_S = \frac{D_L \varepsilon_p C_0 \text{SPDFR}}{K C_0^n} \qquad (15)$$

When the SPDFR is much greater than 1.0 the dominant intraparticle mechanism is surface diffusion. When it is much less than 1.0, pore diffusion dominates. When the SPDFR is 1.0 there is no dominant intraparticle mechanism, i.e., surface diffusion and pore diffusion equally contribute.

The above equations, from Eq. (1) to (15), constitute the PFPSDM. A system of simultaneous partial differential equations is solved by converting the equations to a system of ordinary differential equations by using the method of orthogonal collocation and then integrating by the GEAR method using the subroutine DGEAR [Fridman, 1984].

BACKWASHING MODEL DEVELOPMENT

Unless a prefilter is used, it is common in practice to backwash fixed-bed adsorbers on a regular basis to reduce headloss due to the accumulation of solid particles in the bed. However, backwashing can be detrimental to adsorber performance, as it has been shown to lead to earlier breakthrough [Hong, 1998; Yuasa, 1982].

The liquid and solid phase mass balances for the model development for a backwashed adsorber are the same as those used in the PFPSDM. The only difference is in accounting for backwashing. When the bed is backwashed the adsorbent phase concentrations will be redistributed due to the mixing. Since the new distribution of concentration is not known, the simplest form is to assume that the bed is completely mixed during backwashing, yielding the same solid phase concentration at all depths. Given the particle size and density distribution found with commercially available granular activated carbon (GAC), backwashing a column in practice does not yield a total restratified bed, but results in a very similar particle distribution after each backwashing. Thus, the assumption of completely mixed bed after backwashing is a conservative approach. The solid phase concentrations are averaged axially for each radial coordinate. Therefore, after backwashing each axial coordinate will have the same radial concentration gradient. All solid phase concentrations at each radial position are set to the average concentration, q_i, calculated by Eq. (16).

$$q_i(r, z, t) = \frac{\int_0^L q_i(r, z, t) \, dz}{\int_0^L dz} \qquad (16)$$

The liquid phase concentration after backwashing can be set to the influent concentration (untreated water) or to a zero concentration (treated water). The worst scenario would be to use untreated water, which would give the most conservative results. For this reason, the liquid phase concentration was set to the influent concentration as follows:

$$C_i(z, t) = C_{i0} \qquad (17)$$

The model follows the adsorption equations until the next backwashing process is introduced.

RESULTS AND DICUSSION

1. Sensitivity and Effect of Backwashing for Single Component

Table 1. Input parameters and initial values for sensitivity analysis

C_0	Tortuosity	SPDFR	K	N	MW*	BF*
mg/L	-	-	$(mg/g)(L/mg)^n$	-	daltons	BV*
5.0	1.0	1.0	25	0.2	300	1,000

MW*: Molecular weight
BF*: Backwashing frequency
BV*: Bed volumes

The parameters examined and their starting values are listed in Table 1. Selected parameters were varied one at a time over a range of values to test the response of the model. Sensitivity analysis was simultaneously performed for both the adsorption and the backwashing models. To assess the relative importance of estimating the mass transfer parameters for the fixed bed adsorber, first the single component sensitivity analysis was conducted. The initial parameter values used were determined based on the most general situation: bed porosity, $\varepsilon = 0.45$, void fraction of the pore, $\varepsilon_p = 0.55$, adsorbent density, $\rho_a = 0.856 \, g/cm^3$; equal pore and surface diffusion fluxes, SPDFR=1.0; the diffusion path is equal to particle radius, $\tau = 1.0$; small molecules, MW=300; backwashing every 6.5 days for an adsorber with an 8 min empty bed contact time (EBCT), backwashing frequency (BF) of 1,000 BV; K and n values of a well adsorbed compound, K=25 and n=0.2. The concentration and K values used in section were expressed in terms of dissolved organic carbon. An EBCT of 8 min was used.

Before backwashing, there exists a solid phase concentration distribution in the bed, as well as a bulk liquid solute concentration distribution as shown in Fig. 1. The solid phase concentration distribution within the adsorbent is a function of position in the bed. The bed is gradually exhausted from the top of the column to the bottom of the column without backwashing. However, after backwashing the mass transfer zone no longer exists because of complete mixing of the adsorbent, in which the saturated adsorbent at the top of the
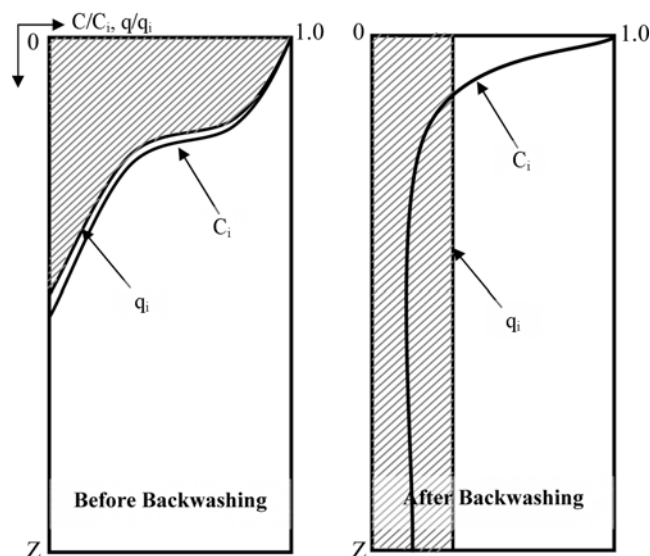

Fig. 1. Comparison of saturated adsorbents distribution before and after backwashing in the fixed bed.
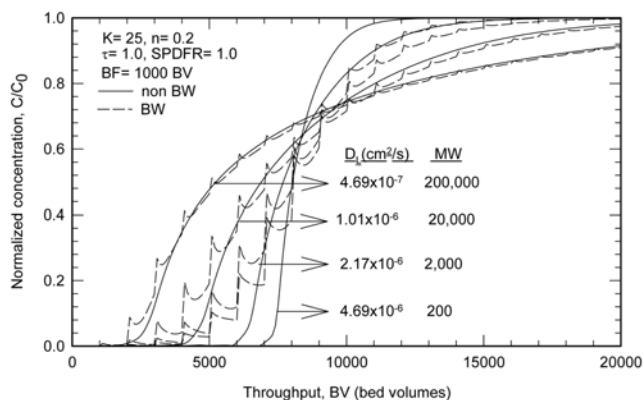
Fig. 2. Imparct of liquid diffusivity or molecular weight on single component breakthrough.
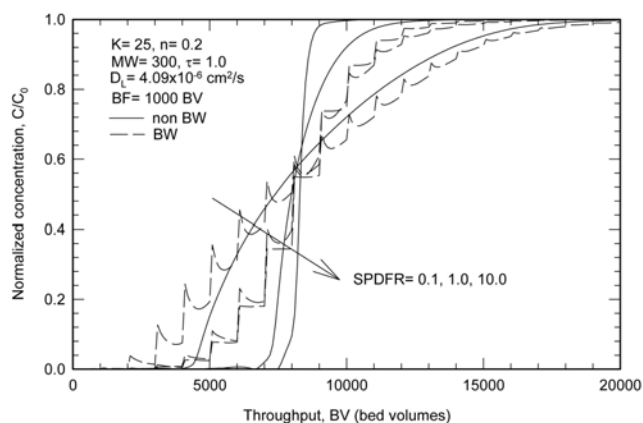

Fig. 3. Impact of surface pore diffusion flux ratio on single component breakthrough.

Fig. 4. Impact of adsorbability on single component breakthrough.

column can be relocated to the bottom of the column. After backwashing, the adsorbate concentration in the liquid phase can be lower than that of the solid phase at the bottom of the column, because the adsorbate concentration in the liquid phase is reduced while passing through the bed. Generally, the backwashed column showed earlier breakthrough due to the reverse adsorbate concentration gradient from the adsorbent to liquid phase at the bottom of the column. The reverse concentration gradient occurred because saturated adsorbents from the top of the column were relocated to the bottom of the column after being completely mixed during backwashing, allowing desorption to take place. This desorption can occur when the adsorption is reversible. The model response to a change in the molecular weight (MW) or liquid diffusivity is shown Fig. 2. The molecular weight was varied from 200 to 200,000. NOM has a molecular weight range of about 1,000 to 100,000. Liquid diffusivity is function of the molecular weight; lower molecular weight indicates faster liquid diffusivity. The liquid diffusivity coefficient was varied from 4.69×10^{-6} to 4.69×10^{-7} cm^2/s. In the PFPSDM, the liquid diffusivity affects both the pore and surface diffusion coefficients. A higher liquid diffusivity results in larger pore and surface diffusion coefficients. Therefore, smaller molecular weight components are transported more quickly through the boundary layer and in the particle compared to the MW components. The lowest MW compound showed a very sharp breakthrough curve. As the MW was increased, the shape of the breakthrough curve to 60 percent breakthrough was broader and indicated earlier breakthrough. The impact of varying the MW was similar for the backwashing model predictions. However, backwashing had a much greater impact on the breakthrough of the smaller MW components, as it resulted in an earlier breakthrough compared to that of the non-backwashed column. This was due to faster diffusivities of the smaller MW compounds, which allowed them quickly diffuse out of the GAC after backwashing. The impact of backwashing decreased as the MW was increased.

Fig. 3 shows the impact of the SPDFR on breakthrough. When surface diffusion dominates, SPDFR>1, the breakthrough pattern is sharper than when pore diffusion dominates, SPDFR<1. Similar tends are seen with the backwashing model prediction, but backwashing always yielded earlier breakthrough for a given SPDFR.

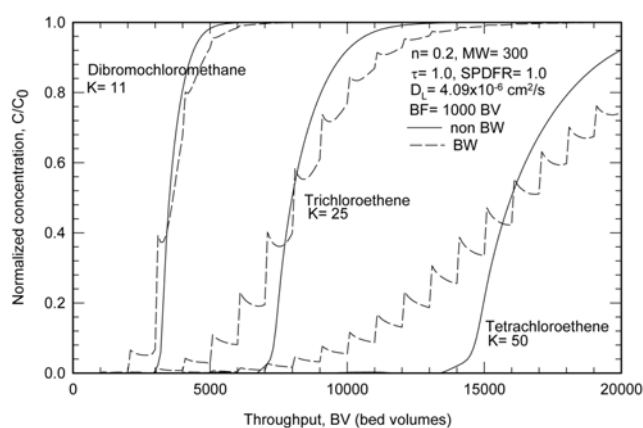Fig. 4 shows the impact of adsorbability and backwashing on

the breakthrough. Each K value represents a common synthetic organic compound in terms of dissolved organic carbon. As expected, the weakly adsorbable component represented by dibromochloromethane, K=11, showed earlier breakthrough compared to the other two components. The impact of backwashing was very similar over the range of adsorbabilities examined. The backwashed column showed at most a 33 percent earlier breakthrough compared to that of the non-backwashed column at 10 percent breakthrough, while backwashing did not show any significant impact on the breakthrough pattern at 50 percent breakthrough.

The model response to a change in backwashing frequency is shown Fig. 5. The backwashing frequency was varied from 300 to 5,000 BV, which represents backwashing every 2 to 30 days for an 8 min EBCT column. Even backwashing at 30 days intervals (BF= 5,000 BV) impacted the breakthrough curve for this K value with a 50 percent breakthrough at 8,000 BV. More frequent backwashing resulted in earlier breakthrough at 10 percent breakthrough; however, there was no significant effect at 50 percent breakthrough. More frequent backwashing showed less impact of backwashing at each backwashing occurrence, because the less saturated adsorbent was relocated to the bottom of the column and less desorption occurred due to the concentration gradient. When the column is backwashed every 50 to 100 BV or more often, the column will behave like a fluidized bed, which means that the mass transfer zone will not exist
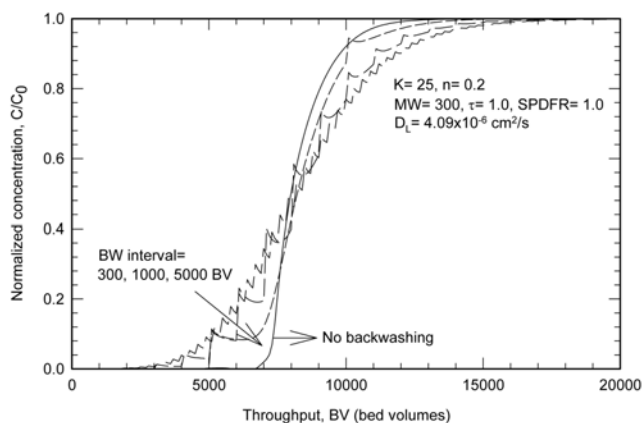
Fig. 5. Impact of backwashing frequency on single component breakthrough.

Table 2. Input parameters and initial values for multi-component sensitivity analysis

C_0	Tortuosity	SPDFR	FCD*	MW*
mg/L	-	-	-	daltons
6.0	7.0	0.1	10 : 10 : 15 : 65	4500

FCD* : Fictive component distribution (K=0, 10, 25, 50)
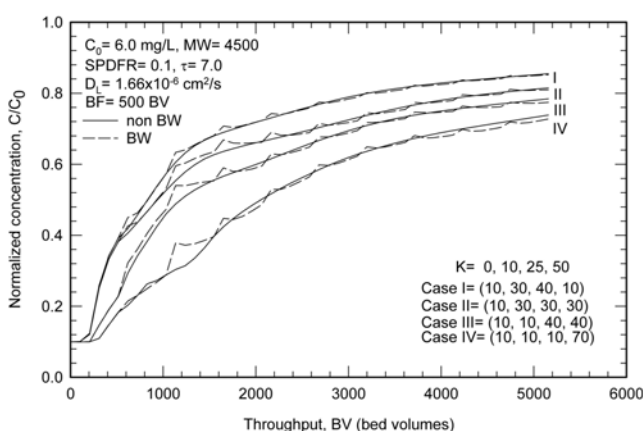MW*: Molecular weight
n=0.2

Fig. 6. Impact of fictive component ratio on multicomponent solution breakthrough.

in the column.

2. Sensitivity and Effect of Backwashing for Multi-component

The parameters and their starting values for a multi-component, such as NOM, are listed in Table 2. Initial parameter values were obtained from previous studies. In this study, the fictive components are divided based on the K values of Freundlich isotherm.

Fig. 6 shows the impact of fictive component composition at the same initial total dissolved organic carbon (DOC) concentration. The concentration distribution of the fictive component fractions was varied similar to that of occurring in natural waters. The non-adsorbable fraction (K=0) was fixed at 10 percent of the initial total DOC concentration. When the solutions contained large amounts
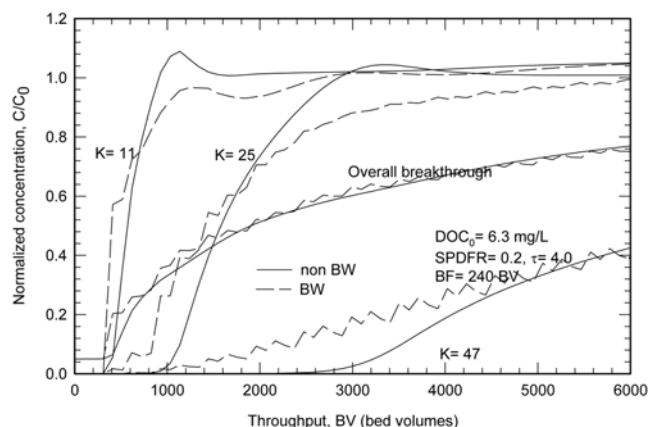

Fig. 7. Fictive component breakthrough and effect of backwashing on multi-components.

of the weakly adsorbable fraction (cases I and II), the breakthrough patterns showed a similar trend up to the 40 percent breakthrough point. After that point, the breakthrough was dictated by the mid-adsorbable and strongly adsorbable fractions. The increasing the amount of the strongly adsorbable fraction in the multi-component solution yielded the later breakthrough.

Fig. 7 shows the breakthrough of each fictive component and overall breakthrough as multicomponent. As seen for the single solute sensitivity analysis, each fictive component of the multi-component solution broke through earlier in the backwashed column compared to the adsorption column. For the multicomponent solution, the earlier breakthrough can be caused by two different reasons: one is the reverse of the concentration gradient and the other is displacement of the weakly adsorbable components on the adsorbent by the strongly adsorbable components. However, the backwashing impact for the multicomponent solution was not significant compared to that for the single component because the breakthrough of each fictive component was staggered and when summed together, the fictive components' behavior at different degrees of breakthrough compensated for the early breakthrough. Thus, further analysis for the multicomponent solution was not performed.

CONCLUSIONS

For the single component sensitivity analysis, the molecular weight was an important parameter. It had a great impact on the single component breakthrough pattern because the low molecular weight compounds had faster liquid diffusivities. The breakthrough of the smaller molecular weight components was impacted significantly by backwashing. Because of their faster diffusivity the compound could diffuse out of the adsorbent after backwashing and appear in the effluent. The SPDFR showed a significant impact on the breakthrough pattern. When surface diffusion was the dominant mechanism, high SPDFR, the breakthrough profile was sharper than when pore diffusion was dominant, low SPDFR. The adsorbability was an important parameter in determining the breakthrough pattern. As expected, the strongly adsorbable component showed a later breakthrough. Backwashing yielded earlier breakthrough for all single components examined. The more frequent backwashing showed the wider breakthrough pattern. The fictive component ratio was an important pa-

rameter in determining the breakthrough pattern in multi-components. When the solution contained more strongly adsorbable component, the fixed bed life was extended. The backwashing impact on the breakthrough pattern of multi-component solutions was not significant for the NOM conditions tested. This was due to staggered breakthrough of each fictive component, and when summed together the fictive component concentrations compensate for each other.

ACKNOWLEDGMENT

NOMENCLATURE

A   : cross sectional area [L^2]
C   : liquid phase concentration [M/L]
$D_{e,i}$: axial eddy dispersitivity [L^2/t]
$D_{p,i}$: pore diffusion coefficient based on pore void fraction [L^2/t]
$D_{s,i}$: surface diffusion coefficient [L^2/t]
D_L : liquid diffusivity [L^2/t]
K   : Freundlich constant $[M/M][L^3/M]^{1/n}$
1/n   : Freundlich constant [dimensionless]
L   : length of fixed bed [L]
M   : mass of adsorbent [M]
q   : solid phase concentration [M/M]
R   : radius of adsorbent [L]
t   : time [t]
v   : interstitial velocity [L/t]
z   : axial coordinate [L]

Greek Letters
ε : void fraction in fixed bed [dimensionless]
ε_p : void fraction in adsorbent [dimensionless]
β_L : film transfer coefficient [L/t]
τ : tortuosity [dimensionless]
ρ_a : adsorbent density [M/L^3]

Subscripts
0   : initial condition
i   : each component
avg : average
p   : pore
s   : surface

REFERENCES

Friedman, G., *Mathematical modeling of multicomponent adsorption in batch and fixed-bed reactors*, MS Thesis, Michigan Technological Univ. Ann Arbor, Michigan. US (1984).

Hong, S., "The role of pH and initial concentration on GAC adsorption for removal of natural organic matter," *J. of Environ. Eng. Res.*, **3**, 183 (1998).

Kim, S. H., Kim, T. W., Cho, D. L., Lee, D. H., Kim, J. C. and Moon, H., "Application of characterization procedure in water and wastewater treatment by adsorption," *Korean J. Chem. Eng.*, **19**, 895 (2002).

Radke, C. J. and Prausnitz, J. M., "Adsorption of organic solutes from dilute aqueous solution on activated carbon," *Ind. Eng. Chem. Fund.*, **11**, 445 (1972).

Randtke, S. J. and Snoeyink, V. L., "Evaluating GAC adsorptive capacity," *J. of AWWA*, **75**, 406 (1983).

Shim, W. G, Chaudhary, D. S., Vigneswaran, S., Ngo, H.-H., Lee, J. W. and Moon, H., "Mathematical modeling of granular activated carbon (GAC) biofiltration system," *Korean J. Chem. Eng.*, **21**, 212 (2004).

Sontheimer, H., Crittenden, J. C. and Summers, R., *Activated carbon for water treatment*, DVGW Forschungsstelle, Karlsruhe, Germany (1988).

Vaith, K., *Predicting the removal of organic carbon with fixed bed adsorbers*, M.S., Thesis, Michigan Technological Univ. Houghton, MI (1988).

Vaith, K., Crittenden, J. C., Hand, D., Wallace, D. E., Aieta, E. M. and Tate, C., *Design of fixed-bed adsorbers to remove natural organic matter*, Proceedings, AWWA Annual Conference, Orlando, FL, June 19-23 (1988).

Yuasa, A., *A kinetic study of activated carbon adsorption processes*, Ph.D Diss., Hokkaido Univ., Sapporo, Japan (1982).